Available online at www.sciencedirect.com
ScienceDirect
Journal of Organometallic Chemistry 692 (2007) 4569–4579
Journal of Organometallic Chemistry
www.elsevier.com/locate/jorganchem

Highly active/selective and adjustable zirconium polymerization catalysts stabilized by aminopyridinato ligands

Winfried P. Kretschmer [a,*], Bart Hessen [a], Awal Noor [b], Natalie M. Scott [b], Rhett Kempe [b,*]

[a] *Center for Catalytic Olefin Polymerization, Stratingh Institute for Chemistry and Chemical Engineering, University of Groningen, Nijenborgh 4, NL-9747 AG Groningen, The Netherlands*
[b] *Lehrstuhl Anorganische Chemie II, University of Bayreuth, 95440 Bayreuth, Germany*

Received 20 March 2007; received in revised form 18 April 2007; accepted 20 April 2007
Available online 6 May 2007

Dedicated to Prof. Gerhard Erker.

Abstract

This paper describes a substantial enhancement of the aminopyridinato ligand stabilized early transition metal chemistry by introducing the sterically very demanding 2,6-dialkylphenyl substituted aminopyridinato ligands derived from (2,6-diisopropylphenyl)-[6-(2,6-dimethylphenyl)-pyridin-2-yl]-amine (**1a**–**H**, ApH) and (2,6-diisopropylphenyl)-[6-(2,4,6-triisopropylphenyl)-pyridin-2-yl]- amine (**1b**–**H**, Ap*H). The corresponding bis aminopyridinato zirconium dichloro complexes, [Ap_2ZrCl_2] (**3a**) and [$Ap_2^*ZrCl_2$] (**3b**) and the dimethyl analogues, [Ap_2ZrMe_2] (**4a**) and [$Ap_2^*ZrMe_2$] (**4b**) (Me = methyl) were synthesized, using standard salt metathesis routes. Single-crystal X-ray diffraction was carried out for the dichloro derivatives. Both zirconium metal centers have a distorted octahedral environment with a *cis*-orientation of the chloride ligands in **3a** and a closer to *trans*-arrangement in **3b**. The dimethyl derivatives are proven to be highly active ethylene polymerization catalysts after activation with [$R_2N(Me)H$][$B(C_6F_5)_4$] (R = $C_{16}H_{33}$–$C_{18}H_{37}$). During attempted co-polymerizations of α-olefins (propylene) and ethylene high activity and selectivity for ethylene and nearly no co-monomer incorporation was observed. Increasing the steric bulk of the ligand going from (2,6-dimethylphenyl) to (2,4,6-triisopropylphenyl) substituted pyridines, switches the catalyst system from producing long chain α-olefins to polymerization of ethylene in a living fashion. In contrast to the dimethyl complexes only [$Ap_2^*ZrCl_2$] in the presence of MAO at elevated temperature gave decent polymerization activity. NMR investigations of the reaction of dichloro complexes with 25 equiv. of MAO or $AlMe_3$ at room temperature revealed, that [Ap_2ZrCl_2] decomposes under ligand transfer to aluminum and formation of [$ApAlMe_2$], while [$Ap_2^*ZrCl_2$] remains almost unreacted under the same conditions. The aminopyridinato dimethyl aluminum complexes, [$ApAlMe_2$] (**5a**) and [Ap^*AlMe_2] (**5b**) were synthesized independently and structurally characterized. The aluminum complexes **5a** and **b** show no catalytic activity towards ethylene, when "activated" with[$R_2N(Me)H$][$B(C_6F_5)_4$].

Keywords: Aluminum; Aminopyridinato ligands; N-ligands; Olefin polymerization; Zirconium

1. Introduction

In recent years the organo zirconium chemistry of the ancillary aminopyridinato ligands (Scheme 1, left) [1] has been increased rapidly. Relatively simple and high yield synthesis, combined with easy modification of steric and electronic properties of the precursor aminopyridines have led to a wide variety of mono, bis, tris and tetrakis aminopyridinato derivatives. In general, aminopyridinato ligands are interesting non-symmetric versions of bidentate monoanionic N-Ligands suited to stabilize early and late transition metals and can be considered as related to amidinates [2] or NacNac [3] ligands (Scheme 1, middle and right, respectively).

* Corresponding authors. Tel.: +49 921552540.
E-mail addresses: W.P.Kretschmer@rug.nl (W.P. Kretschmer), Kempe@Uni-Bayreuth.de (R. Kempe).

0022-328X/$ - see front matter © 2007 Elsevier B.V. All rights reserved.
doi:10.1016/j.jorganchem.2007.04.041

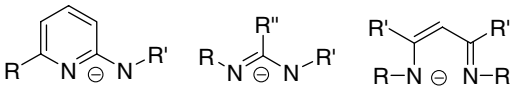

Scheme 1. Aminopyridinato ligands (left) and other related bidentate monoanionic N-Ligands (R, R′ and R″, for instance, alkyl or aryl substituents).

However, comparing with the literature only a few aminopyridinato ligand based zirconium olefin polymerization catalyst systems, with low or moderate activity have been reported. It seems that the olefin polymerization chemistry of the aminopyridinato zirconium complexes has been limited so far since no ligands were available that could avoid ligand redistribution to tris or tetrakis aminopyridinato complexes independent from the ''remaining'' ligands [4]. Contributions by Scott and co-workers emphasize the importance of the introduction of steric bulk at the pyridine ring [4f,4g]. Thus, we concluded that the bulky aminopyridinato ligands containing 2,6-disubstituted phenyl substituents at the amido N-atom and at the pyridine ring introduced by us recently [5] could address this problem.

In this contribution, we report the synthesis of zirconium polymerization catalysts based on sterically very demanding aminopyridines (2,6-diisopropylphenyl)-[6-(2,6-dimethylphenyl)-pyridin-2-yl]-amine (**1a**–**H**, ApH) and (2,6-diisopropylphenyl)-[6-(2,4,6-triisopropylphenyl)-pyridin-2-yl]- amine (**1b**–**H**, Ap*H) (Scheme 2). It is shown that such zirconium aminopyridinato complexes are thermally robust and highly active ethylene polymerization catalysts. Furthermore, a selective discrimination of propylene in ethylene/propylene-copolymerization is observed. Such monomer selectivity especially in combination with high temperature stability could be of relevance for instance in chain shuttling polymerizations [6]. Furthermore, the increase of steric bulk going from Ap to Ap* switches the catalyst system from producing long chain α-olefins to polymerization of ethylene in a living fashion, if no chain transfer agents are present. The introduction of bulkiness does not necessarily lead to very high polymerization activity of the corresponding metal complexes. For related, sterically demanding amidinate-based zirconium catalysts only low activities were observed [7].

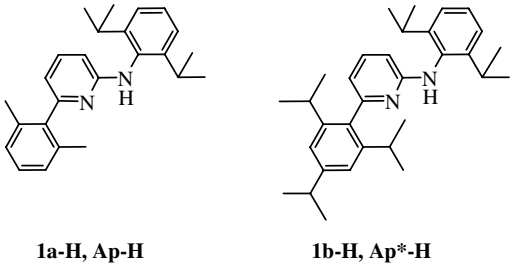

1a-H, Ap-H **1b-H, Ap*-H**

Scheme 2. 2,6-Dialkylphenyl substituted amino pyridines.

2. Results and discussion

2.1. Synthesis and characterization of the zirconium dichloride and dimethyl complexes

The reaction of the potassium salts **2a/b** [5a] with $ZrCl_4$ leads to the zirconium dichlorides **3a/b** which on reacting with methyl lithium convert selectively to the bisalkyls **4a/b** (Scheme 3).

The molecular structures of **3a/b** were determined via X-ray crystal structure analysis (for experimental details see Table 1) and are shown in Fig. 1. The space filling model clearly indicates a well protected active site of **3b** compared to **3a**. The overall coordination environment of complexes **3a/b** can best be described as distorted octahedron with *cis* orientated chlorides for **3a** [96.47(4)°], while the Cl–Zr–Cl angle of **3b** is significantly closer to a transoide arrangement [123.08(6)°]. The differences in the Zr–N_{amido}/Zr–$N_{pyridine}$ bond lengths indicate a localized binding mode. The anionic charge of the N ligand is localized at the N_{amido} atom which means a classic donor functionalized amido metal bond rather than an aminopyridinate is observed [8].

Despite the bulk of the ligands and their crowded metal environment the aminopyridinato complexes **3a/b** and **4a/b** show a dynamic behaviour in solution. In the ^1H and ^{13}C NMR spectra at room temperature for all four complexes only one set of resonances for both ligands is observed (see for instance Fig. 3a). These together with the splitting of the methyl resonances for each isopropyl group in a doublet of doublets indicates, there is a chemically difference for the upper and lower site of the aromatic rings while the right and left is equal. This observation indicates a fast inter-conversion of the ligands on NMR timescale at room temperature. Reaction of **4b** with *N*,*N*-dimethylanilinium-tetra(pentafluorophenyl)borate ($[PhNMe_2H][B(C_6F_5)_4]$) in bromobenzene leads to the corresponding $[Ap^*_2ZrMe]^+$ cation (Scheme 4).

Despite the increase in space around the metal (abstraction of one of the alkyl functions) the increase in electrostatic interaction between the cationic metal center and the pyridine fragment most likely prevents the dissociation and leads to five chemically unequal isopropyl groups (Fig. 3b). This observation is indicative of a dissociative

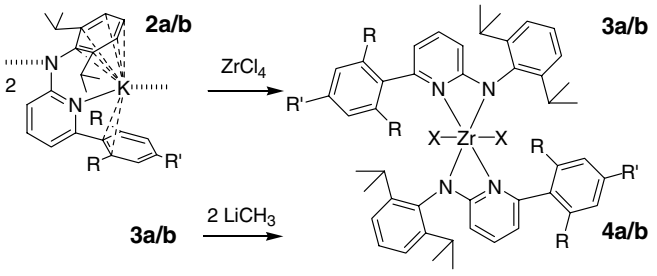

Scheme 3. Synthesis of **3a/b** and **4a/b** (**3**: X = Cl, **4**: X = CH_3; **a**: R = Me, R′ = H; **b**: R, R′ = *i*-Pr).

Table 1
Details of the X-ray crystal structure analyses of **3a** * $2C_6D_6$, **3b** * C_6H_{14}, **5a** and **5b**

Compound	**3a** * $2C_6D_6$	**3b** * C_6H_{14}	**5a**	**5b**
Formula	$C_{59}H_{67}Cl_2N_4Zr$	$C_{67}H_{93}Cl_2N_4Zr$	$C_{27}H_{35}AlN_2$	$C_{34}H_{49}AlN_2$
Molecular weight	994.29	1116.57	414.55	512.73
Crystal system	Triclinic	Triclinic	Orthorhombic	Triclinic
Space group	$P\bar{1}$	$P\bar{1}$	*Pbca*	$P\bar{1}$
a (Å)	10.620(1)	12.191(1)	15.3010(12)	10.9320(10)
b (Å)	12.217(1)	13.561(2)	17.4760(13)	12.0050(10)
c (Å)	20.789(2)	20.431(2)	18.9130(17)	13.4470(11)
α (°)	91.276(5)	106.085(5)	90.000(7)	75.446(7)
β (°)	97.303(6)	91.940(5)	90.000(7)	81.462(7)
γ (°)	95.911(5)	91.558(5)	90.000(6)	70.393(7)
V (Å^3)	2659.4(8)	3241(1)	5057.3(7)	1605.1(2)
Z	2	2	8	2
Crystal size (mm^3)	$0.15 \times 0.12 \times 0.10$	$0.24 \times 0.09 \times 0.06$	$0.42 \times 0.35 \times 0.23$	$0.45 \times 0.36 \times 0.25$
Habit	Prism	Needle-like	Prism	Prism
Color	Yellow	Yellow	Yellow	Colorless
ρ_{calc} (g cm^{-3})	1.242	1.144	1.089	1.061
T (K)	193(2)	193(2)	193(2)	193(2)
θ Range (°)	1.68–25.84	1.56–26.35	1.33–26.03	1.57–26.06
Reflections unique	10196	12821	4813	6076
Reflections observation ($I > 2\sigma(I)$)	6736	3466	2908	3733
Number of parameters	595	652	271	334
wR^2 (all data)	0.1381	0.0918	0.1537	0.1113
R value ($I > 2\sigma(I)$)	0.0543	0.0414	0.0705	0.0507

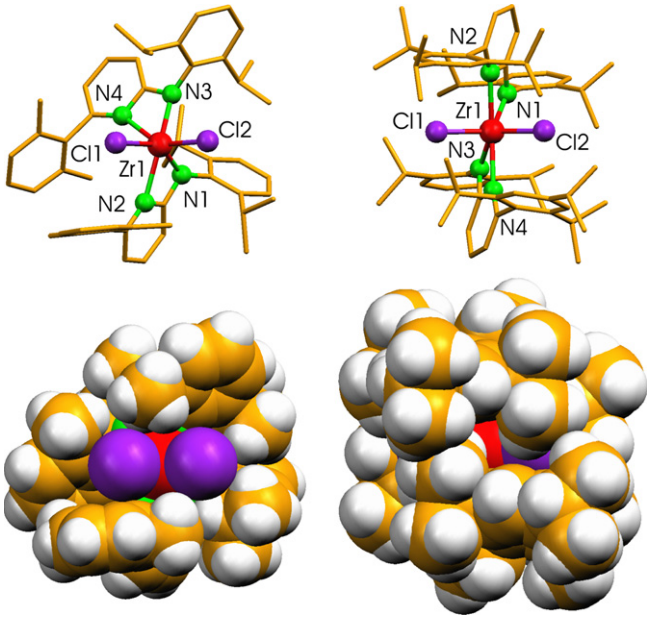

Fig. 1. Molecular structures of **3a** (left) and **3b** (right). Selected bond lengths [Å] and angles [°]: **3a** Zr1 N3 2.123(3), Zr1 N1 2.145(3), Zr1 N4 2.348(3), Zr1 N2 2.355(3); N3 Zr1 N4 60.04(11), N1 Zr1 N2 59.44(11), Cl2 Zr1 Cl1 96.47(4); **3b** N1 Zr1 2.154(4), N2 Zr1 2.358(4), N3 Zr1 2.184(4), N4 Zr1 2.338(4); N3 Zr1 N4 59.40(14), N1 Zr1 N2 59.52(14), Cl1 Zr1 Cl2 123.08(6).

mechanism of the exchange process observed for **3a/b** and **4a/b** (Fig. 2). It is notable that reaction of **4b** with tris(pentafluorophenyl)borane give identical ^{1}H and ^{13}C NMR spectra in bromobenzene except the resonances for the dimethylaniline and the different anions. The formation of solvent separated cation–anion-pairs through smooth methyl abstraction was also reflected by the small value of $\Delta\delta$[(*p*-F)-(*m*-F)] of 2.4 ppm [9].

2.2. Olefin polymerization and formation of aluminum aminopyridinates

Despite the fact that the difference in the aminopyridinato ligands Ap and Ap* is quite small, the influence on the polymerization activity of their complexes **3a** and **b** if activated with MAO was found to be huge. As shown in Table 2 activated **3b** polymerizes ethylene highly actively [10] at elevated temperature. Ethylene consumption was observed over the whole time period (15 min). Complex **3a** was almost inactive after a few minutes under the same conditions. To gain more insight into this different behaviour we studied the stability of **3a** and **3b** against d-MAO ("dry methylaluminoxane") in NMR tube experiments. NMR tubes were charged with 10 μmol of dichloride **3a/b** in 0.5 ml of deutero-benzene before 25 equiv. of d-MAO were added. While **3b** reacts smoothly (50% in 24 h) with MAO to form the corresponding methyl complex, compound **3a** shows a fast decomposition to insoluble products and ligand transfer to aluminum (Scheme 5, Fig. 4). After 5 min an NMR detectable amount of [ApAlMe$_2$] (**5a**) was found. After 6 h **5a** seems to be the only Ap containing species present. To prove this observation we independently synthesized the aminopyridinato containing dimethyl aluminum complexes [ApAlMe$_2$] (Scheme 6, **5a**) and [Ap*AlMe$_2$] (**5b**), by reaction of the aminopyridines **1a–H** and **1b–H** with TMA (trimethylaluminum) in toluene. Removal of all volatiles under reduced pressure give the spectroscopically pure products as colorless oils, which

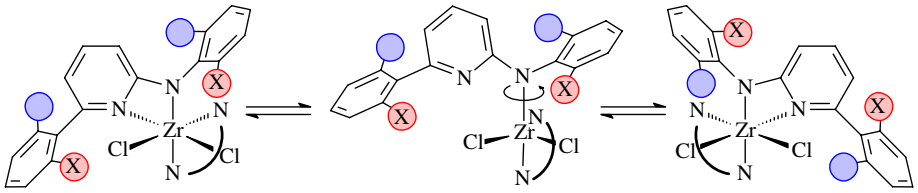

Fig. 2. Proposed reaction mechanism for the dissociative inter-conversion.

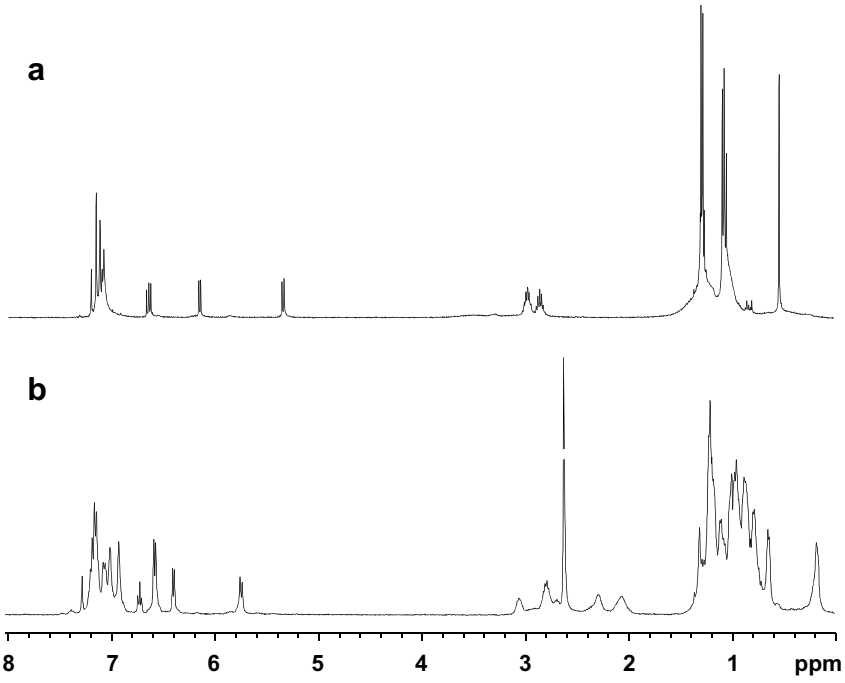

Fig. 3. ^{1}H NMR spectrum of $[Ap^*_2ZrMe_2]$ (a) (C_6D_6, 20 °C) and after addition of 1 equiv. $[PhNMe_2H][B(C_6F_5)_4]$ (b) (C_6D_5Br, 20 °C).

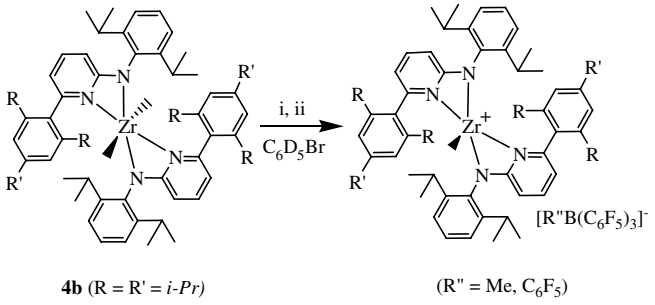

4b (R = R' = *i-Pr*) (R" = Me, C_6F_5)

Scheme 4. Formation of the alkyl zirconium cations through reaction with (i) $B(C_6F_5)_3$ and (ii) $[PhNMe_2H][B(C_6F_5)_4]$.

could be crystallized by very slow evaporation of hexane solutions. The crystal structures are presented in Fig. 5. Experimental details of the analyses can be found in Table 1. Both structures are mononuclear involving a strained η^2 coordination of the Ap ligand. The Al–N bond distances are quite similar and thus indicative of a binding mode with a high degree delocalization of the anionic function of the Ap ligands. η^2 coordinated Ap aluminum complexes are rare [5c,11,12]. The first compound of this kind was published by Wang and coworkers [12].

Table 2
Temperature dependence of the ethylene polymerization catalyzed by **3a/b** (activation with MAO)[a]

pre-cat.	T (°C)	Activator	m_{Pol} (g)	Activity ($kg_{PE}\ mol_{cat}^{-1}\ h^{-1}\ bar^{-1}$)	M_w (g mol^{-1})	M_w/M_n
3a	50	MAO	0.7	280	790 000	35.3
3a	80	MAO	0.8	320	675 000	14.6
3b	30	MAO	0.4	160	890 800	15.1
3b	50	MAO	1.7	680	835 200	3.1
3b	80	MAO	6.9	2760	535 500	2.0
3b	100	MAO	6.7	2680	392 300	2.2
3b[b]	50	MAO	5.9	2360	541 500	1.9

[a] pre-cat.: 2 μmol, Zr/Al = 1/500, 260 ml toluene, pressure: 5 bar, t: 15 min.

[b] Ten minutes of premixing of **3b** with 250 equiv. of MAO in 2 ml of toluene (over all Zr/Al = 1/500).

The temperature dependence of the polymerization activity of **3a/b** if activated with MAO is shown in Table 2. Complex **3b** activated with MAO gives rise to a highly active single site catalyst. No ligand redistribution which can give rise to additional polymerization active species seems to occur during the polymerization process as can be seen from the narrow molecular weight

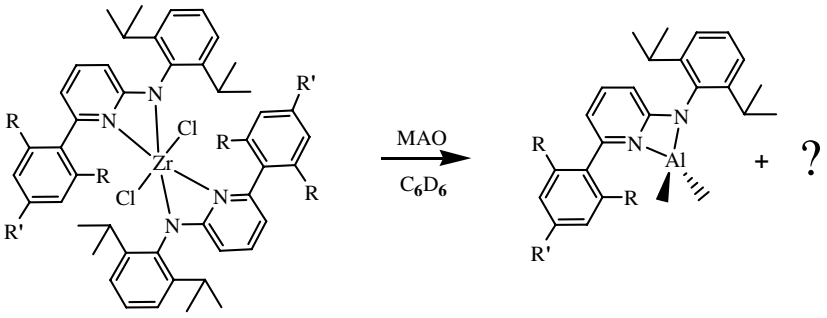

3a(R'= H,R =Me)
3b(R =R' = *i-Pr*)

5a(R' =H,R=Me)
5b(R =R' = *i-Pr*)

Scheme 5. MAO assisted aminopyridinato ligand transfer from Zr to Al.

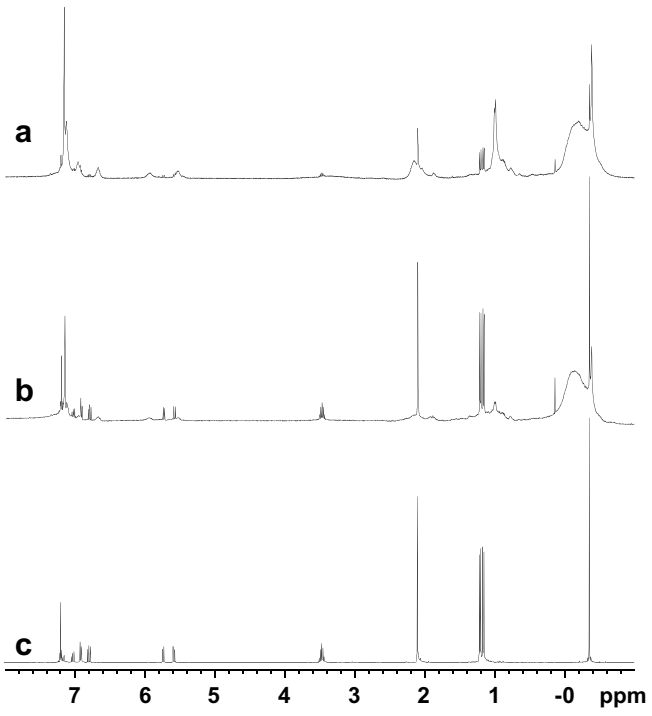

Fig. 4. ^{1}H NMR spectra (C_6D_6, 20 °C) of [Ap_2ZrCl_2] + 25 equiv. d-MAO (a) after 5 min and (b) after 6 h. (c) ^{1}H NMR spectrum (C_6D_6, 20 °C) of [$ApAlMe_2$].

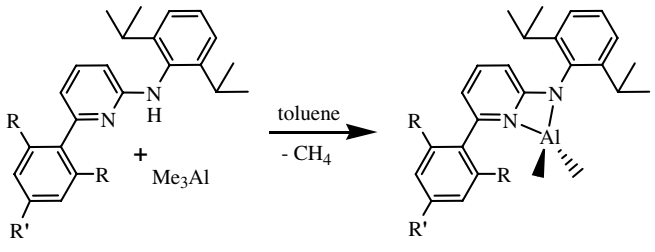

5a (R' = H, R = Me)
5b (R = R' = *i-Pr*)

Scheme 6. Synthesis of **5a/b**.

distributions. The low activity at low temperature results mainly from a very slow alkylation due to the poor accessibility of the two chloro ligands (Fig. 1) which was also reflected in the decrease of the induction periods with increasing temperature. Induction periods (time between injection of the pre-catalyst and start of the ethylene uptake) of about 120 s at 30 °C, 75 s at 50 °C and 25 s at 80 °C were observed. The slow alkylation, especially at low temperatures, is also in accordance with the rather broad polydispersity observed for the 30 °C run in comparison to the higher temperature runs. A possibility to overcome the slow alkylation problem is the premixing of **3b** with an excess of MAO prior to injection (Table 2, entry 7). It is also notable that the catalyst system is very robust at elevated temperatures since a very high activity is observed even at 100 °C as well. Ethylene consumption for this run had been observed during the entire polymerization process (15 min) (Table 2, entry 6).

Since ligand transfer processes seems to interfere while alkylation seems to be rate limiting, we became interested in perfluoroarylborate activation protocols. The abstraction of one of the two methyl groups of **4a/b** by ammonium perfluorotetraphenylborate leads to highly active polymerization catalyst systems. Again a notable difference was found between the Ap and Ap* containing catalysts. In contrast to the **3a**/MAO catalyst system **4a** (after activation with ammonium perfluorotetraphenylborate) was found to be highly active in the formation of long chain α-olefins (Fig. 6) indicating a rather fast β-H-elimination/transfer. Molecular weight distribution clearly shows the presence of a single site catalyst, while no ligand transfer to scavenger was observed. The more crowded pre-catalyst **4b** [13] instead gives high molecular weight polyethylene most likely due to sterically disfavored direct β-H transfer [14,15]. However, under the applied conditions only multimodal distributed polymers were found (Fig. 7). The GPC data are also indicative of a rather narrowly distributed main peak. The rapid precipitation of the polymers may lead to a diffusion controlled process and thus to the broad molecular weight distribution. This problem could be addressed by a reduction of the catalyst concentration.

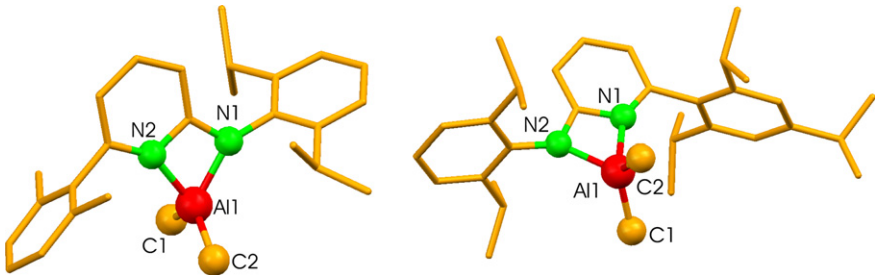

Fig. 5. Molecular structures of **5a** (left) and **5b** (right). Selected bond lengths (Å) and angles (°): **5a** Al1 N1 1.922(2), Al1 N2 1.959(2), Al1 C1 1.944(3), Al1 C2 1.954(3); N1 Al1 N2 68.87(10), C1 Al1 C2 120.69(16); **5b** Al1 N1 1.9212(18), Al1 N2 1.9855(17), Al1 C1 1.941(2), Al11 C2 1.943(2); N1 Al1 N2 68.63(7), C1 Al1 C2 119.98(12).

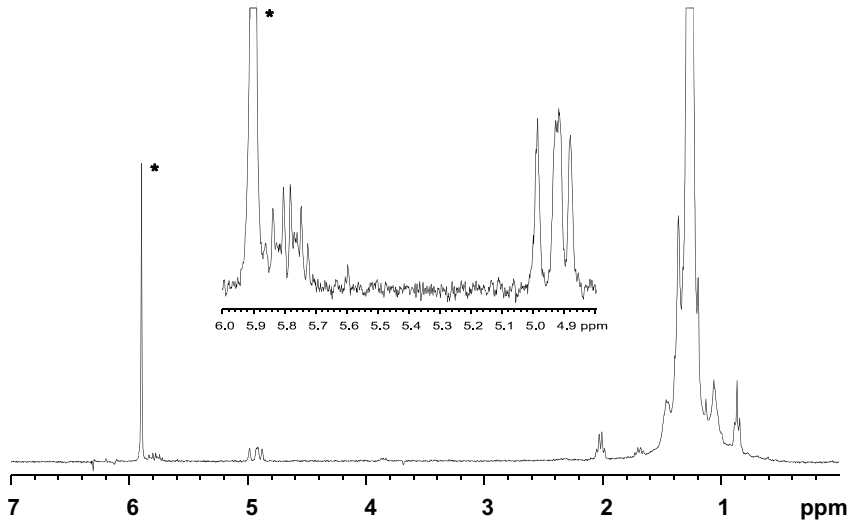

Fig. 6. ^{1}H NMR spectrum (*$C_2D_2Cl_4$, 120 °C) of PE (Table 3, entry 3).

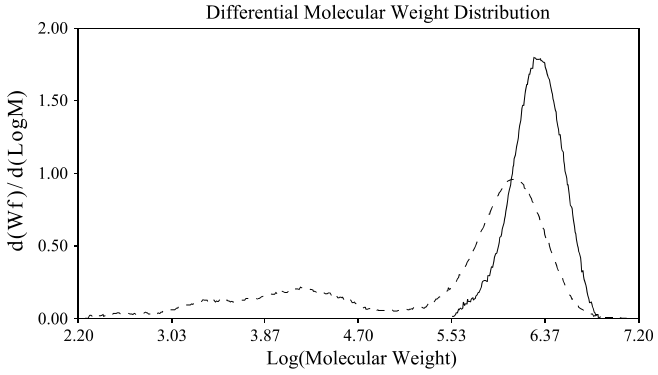

Fig. 7. Molecular weight distribution (SEC) of the polymerization experiments listed in Table 3, entry 6 and Table 4, entry 3.

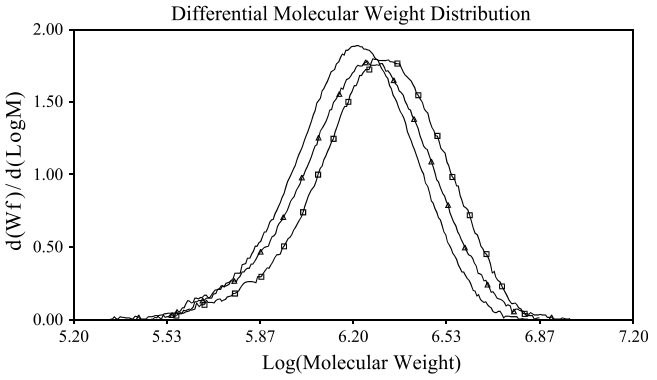

Fig. 8. Molecular weight distribution (SEC) of the polymerization experiments listed in Table 4.

Consequently, under a regime which avoids diffusion controlled circumstances a "living" polymerization process (Table 4, Fig. 8) is observed [16]. As long as the living chains stay in solution very fast chain growing (for the first seconds) was evidenced by a high ethylene consumption. At some stage the polymer precipitates, ethylene consumption drops down and we observe further chain growing of the precipitated polymer. This part of the chain growing process is shown in Table 4, Fig. 8.

The catalyst systems based on **3a/b** (activation with MAO) or **4a/b** (borate activation) are not active towards α-olefins (for instance propylene) [17]. Catalysts that polymerize ethylene and for which olefin insertion is blocked in the presence of α-olefins are well documented. Such a behaviour is observed for instance for lanthanide catalysts [18]. A variety of transition metal complexes get into a dormant state in the presence of α-olefins. Ethylene is able to reactivate the catalyst which leads to specific insertion

sequences [19]. Both mechanisms are not valid for the catalysts systems described here as can be seen from experiments in which the catalysts are exposed to a mixture of ethylene and propylene (Table 3, entry 9 and 10). Even at relatively high partial propylene pressure ethylene is polymerized selectively. NMR spectroscopy of the obtained polymers revealed a propylene insertion of less than 1 mol%. Polymer data are quite similar if carried out in the absence or presence of propylene (Table 3, entries 3 and 9). A highly selective polymerization of ethylene out of an ethylene/propylene mixture seems to be possible. Such a behaviour can result from steric or electronic characteristics. If steric reasons dominate one could describe it as shape selectivity as documented for micro porous materials like zeolites [20]. We concluded that the electronic situation at the metal centre caused by the Ap ligands is dominating the responsibility for such a behaviour since the selectivity is observed for **3/4a** and **b** and not just for the significantly higher crowded zirconium moieties (Fig. 1). Steric reasons are most likely responsible for the product selectivity – the selective formation of either α-olefines (Ap_2Zr alkyl cations) or saturated products attached at the Zr centre in a living fashion or chain transferred to Al if aluminum alkyls are present (in case of Ap^*_2Zr alkyl cations).

Table 3
Temperature dependence of the ethylene polymerization catalyzed by **4a/b** (activation with ammonium perfluorotetraphenylborate)[a]

pre-cat.	T (°C)	m_{Pol} (g)	Activity ($kg_{PE}\ mol_{cat}^{-1}\ h^{-1}\ bar^{-1}$)	M_w ($g\ mol^{-1}$)	M_w/M_n
4a	30	1.9	760	12070	2.3
4a	50	4.9	1960	10900	2.1
4a	80	11.1	4440	9670	1.9
4a	100	7.0	2800	9000	2.0
4b	30	3.5	1400	1833000	22.5[b]
4b	50	6.3	2520	1371000	29.8[b]
4b	80	7.9	3160	1063000	393.7[b]
4b	100	9.4	3760	1009000	176.7[b]
4a[c]	80	27.0	54000[d]	8960	2.2
4b[c]	80	28.5	57000[d]	755700	113.1[b]

[a] pre-cat.: 2 μmol, ammoniumborate: $[R_2N(CH_3)H]^+[B(C_6F_5)_4]^-$ ($R = C_{16}H_{33}$–$C_{18}H_{37}$), Zr/B = 1/1.1, **4** and borate were mixed prior to the injection, scavenger: TIBAO (tetra-*iso*-butyl-aluminoxane), Zr/Al = 1/50, 260 ml toluene, pressure: 5 bar, *t*: 15 min.
[b] multimodal.
[c] co-polymerization, pressure: 5 bar propylene, 15 bar total.
[d] $kg_{PE}\ mol_{cat}^{-1}\ h^{-1}$.

Table 4
Living ethylene polymerization at 50 °C

t (min)	m_{Pol} (g)	Activity ($kg_{PE}\ mol_{cat}^{-1}\ h^{-1}\ bar^{-1}$)	M_w ($g\ mol^{-1}$)	M_w/M_n
3	0.46	9200	1745000	1.26
9	0.67	4467	1996000	1.33
15	0.88	3520	2301000	1.30

4b: 200 nmol, ammoniumborate: $[R_2N(CH_3)H]^+[B(C_6F_5)_4]^-$ ($R = C_{16}H_{33}$–$C_{18}H_{37}$), Zr/B = 1/1.1, **4b** and borate were pre-mixed prior the injection, scavenger: TPPAO {tetra-(2-phenyl-1-propyl)aluminoxane}, Zr/Al = 1/500, 260 ml toluene, pressure: 5 bar, *T*: 50 °C.

3. Conclusions

Several conclusions can be drawn from this study. First, the ligands used here namely Ap and Ap* are able to avoid ligand redistribution to tris or tetrakis aminopyridinato zirconium complexes independent from the ''remaining'' ligands due to steric demand. Second, the zirconium complexes are thermally robust, highly active and selective ethylene polymerization catalysts. Out of a mixture of ethylene and propylene, ethylene is polymerized highly selectively. Third, slight changes in the steric demand of the bulky ligand periphery can be used to tune the nature of the formed polymers by maintaining the selectivity issue. Fourth, Ap^*_2Zr alkyl cations can polymerize ethylene in a living fashion even at 50 °C.

4. Experimental

4.1. General aspects

All reactions were carried out under inert atmosphere using standard glove box and Schlenk line techniques. The solvents toluene, pentane, hexane, diethyl ether, and tetrahydrofurane were dried by refluxing over sodium/benzophenone. Benzene-d_6 was dried over sodium/potassium alloy and bromobenzene-d_5 over molecular sieves. Toluene for polymerization (Aldrich, anhydrous, 99.8%) was passed over columns of Al_2O_3 (Fluka), BASF R3-11 supported Cu oxygen scavenger and molecular sieves (Aldrich, 4 Å). Ethylene (AGA polymer grade) was passed over BASF R3-11 supported Cu oxygen scavenger and molecular sieves (Aldrich, 4 Å). *N*,*N*,*N*-Trialkylammonium(tetrapentafluorophenyl)borate ($[R_2NMeH][B(C_6F_5)_4]$, $R = C_{16}H_{33}$–$C_{18}H_{37}$, 6.2 wt.% $B(C_6F_5)_4^-$ in Isopar, DOW Chemicals), trimethyl aluminum (TMA, 2.0 M in toluene, Aldrich), TIBA (Witco), and polymethylaluminoxane ($[MeAlO]_n$, PMAO, 4.9 wt.% in Al, Akzo) were used as received. Tetra-*iso*-butyl aluminoxane ($[i\text{-}Bu_2Al]_2O$, TIBAO) and tetra(2-phenyl-1-propyl) aluminoxane ($\{[CH_3CH(Ph)CH_2]_2Al\}_2O$, TPPAO) were prepared according to published procedure [21]. d-MAO was prepared by removal of all volatile from PMAO (4.9 wt.% in Al, Akzo). The synthesis of **1a**–**H**, **1b**–**H**, **2a** and **2b** has been described previously [5a].

NMR spectra were recorded on a Varian Gemini 400 (^1H: 400 MHz, ^{13}C: 100.5 MHz) or Varian VXR-300 (^1H: 300 MHz, ^{13}C: 75.4 MHz) or a Bruker ARX 250 (^1H: 250 MHz, ^{13}C: 63 MHz) spectrometer. The ^1H and ^{13}C NMR spectra, measured at 25 °C and 120 °C, were referenced internally using the residual solvent resonances, and the chemical shifts (δ) reported in ppm. The polymer samples were prepared by dissolving 15 mg of the polymer in 0.5 ml $C_2D_2Cl_4$ at 100 °C for 3 h before measuring. Gel permeation chromatography (GPC) analysis was carried out on a Polymer Laboratories Ltd. (PL-GPC210)

chromatograph, equipped with a capillary differential viscometer (Viscotek), a refractive index (RI) detector and a two-angle (15° and 90°) light scattering photometer at 150 °C using 1,2,4-trichlorobenzene as the mobile phase. The samples were prepared by dissolving the polymer (0.1% weight/volume) in the mobile phase solvent in an external oven and were run without filtration. The molecular weight was referenced to polyethylene ($M_w = 50\,000$ g/mol) and polystyrene ($M_w = 100\,000$–$500\,000$ g/mole) standards. The reported values are the average of at least two independent determinations. X-ray crystal structure analysis was carried out at a STOE IPDS II diffractometer equipped with an Oxford Cryostream low temperature unit.

4.2. General description of ethylene polymerization experiments with MAO

The catalytic ethylene polymerization reactions were performed in a stainless steel 1 L autoclave (Medimex) in semi-batch mode (ethylene was added by replenishing flow to keep the pressure constant). The reactor was temperature and pressure controlled and equipped with separated toluene, catalyst and co-catalyst injection systems and a sample outlet for continuous reaction monitoring. Up to 15 bar of ethylene pressure multiple injections of the catalyst with a pneumatically operated catalyst injection system were used. During a polymerization run the pressure, the ethylene flow, the inner and the outer reactor temperature and the stirrer speed were monitored continuously. In a typical semi-batch experiment, the autoclave was evacuated and heated for 1 h at 125 °C prior to use. The reactor was then brought to desired temperature, stirred at 600 rpm and charged with 230 ml of toluene together with PMAO (550 mg of a toluene solution, 4.9 wt.% Al, 1 mmol), if not mentioned different in the text. After pressurizing with ethylene to reach 5 bar total pressure the autoclave was equilibrated for 5 min. Subsequently 1 ml of a 0.002 M catalyst stock solution in toluene was injected together with 30 ml of toluene, to start the reaction. During the run the ethylene pressure was kept constant to within 0.2 bar of the initial pressure by replenishing flow. After 15 min reaction time the reactor was vented and the residual aluminum alkyls were destroyed by addition of 100 ml of ethanol. Polymeric product was collected, stirred for 30 min in acidified ethanol and rinsed with ethanol and acetone on a glass frit. The polymer was initially dried on air and subsequently in vacuum at 80 °C.

4.3. Description of ethylene polymerization experiments with ammonium borate activator

The general procedure and conditions as described above were followed, using 1 ml of a 0.05 M solution of TIBAO (tetra-*iso*-butyl-aluminoxan, Zr/Al = 1/50) in toluene instead of PMAO to charge the reactor and a catalyst mixture instead of the stock solution to start the reaction. The catalyst mixture was prepared by successively adding 1 ml of toluene and 1 ml of a 0.002 M catalyst stock solution in toluene to 25 mg of $[R_2NMeH][B(C_6F_5)_4]$ ($R = C_{16}H_{33}$–$C_{18}H_{37}$, 6.2 wt.% $B(C_6F_5)_4^-$ in Isopar, Zr/B = 1/1.1). After shaking for 1 min the mixture was injected, to start the reaction.

Alternatively, 1 ml of a 0.05 M solution of TPPAO (tetra(2-phenyl-1-propyl)aluminoxane, Zr/Al = 1/500) in toluene instead of TIBAO and a catalyst mixture prepared by successively adding 1 ml toluene and 100 μl of a 0.002 M catalyst stock solution toluene to 2.5 mg of $[R_2NMeH][B(C_6F_5)_4]$ ($R = C_{16}H_{33}$–$C_{18}H_{37}$, 6.2 wt.% $B(C_6F_5)_4^-$ in Isopar, Zr/B = 1/1.1) were used.

4.4. Description of ethylene/propylene co-polymerization experiments

The general procedure and conditions as described above were followed, using successively 5 bar propylene and 15 bar ethylene to pressurize the reactor.

4.5. Synthesis of the metal complexes

4.5.1. Synthesis of **3a**

THF (40 ml) was added to $[ZrCl_4(THF)_2]$ (0.38 g, 1.00 mmol) and **2a** (0.80 g, 2.00 mmol), in a Schlenk vessel and the mixture was stirred for 15 h. The solvent was removed in vacuum and hexane (30 ml) was added. The bright yellow reaction mixture was filtered and the filtrate was allowed to stand at room temperature for 24 h to afford yellow crystals. Yield: 0.52 g (54%). Elemental analyses for $C_{50}H_{58}Cl_2N_4Zr$ (877.15): C, 68.5; H, 6.7; N, 6.4. Found: C, 68.1; H, 7.1; N, 6.4%.

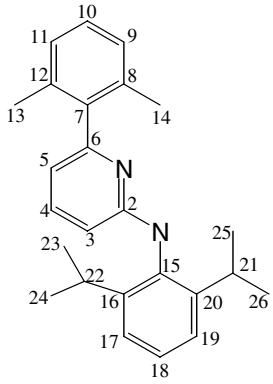

3a: ^{1}H NMR: (250 MHz, C_6D_6, 298 K): $\delta = 0.87$–1.21 (m, 24H, $H^{24,25,26,27}$), 2.09 (v br s, 12H, $H^{13,14}$), 3.28 (br m, 4H, $H^{21,22}$), 5.52 (br d, 2H, H^3), 5.87 (br d, 2H, H^5), 6.67 (t, 2H, H^4), 6.98–7.13 (m, 12H, $H^{9,10,11,17,18,19}$). ^{13}C NMR (63 MHz, C_6D_6, 298 K): $\delta = 20.50$ ($C^{13,14}$), 23.83 ($C^{21,22}$), 28.72 ($C^{23,24/25,26}$), 30.18 ($C^{23,24/25,26}$), 103.73 (C^3), 114.55 (C^5), 124.19 ($C^{9,11}$), 126.88 ($C^{18/10}$), 127.78 ($C^{17,19}$), 134.70 ($C^{8/10}$), 135.88 ($C^{8,12}$), 137.86 (C^7), 141.85 (C^4), 144.84 (C^{15}), 148.03 ($C^{16,20}$), 159.30 (C^6), 159.90 (C^2) ppm.

*4.5.2. Synthesis of **3b***

This compound was obtained in the same way as **3a**, with **2b** (0.99 g, 2.00 mmol) instead of **2a**. Yield: 0.60 g (56%). Elemental analyses for $C_{64}H_{86}Cl_2N_4Zr$ (1073.52): C, 71.6; H, 8.1; N, 5.2. Found: C, 71.4; H, 8.2; N, 4.7%.

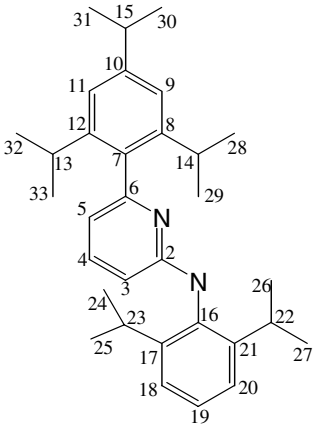

3b: ^{1}H NMR (250 MHz, C_6D_6, 298 K): $\delta = 0.99$–1.37 (m, 60H, $H^{24,25,26,27,28,29,30,31,32,33}$), 2.89–3.05 (m, 6H, $H^{13,14,15}$), 3.34 (sep, 4H, $H^{22,23}$), 5.39 (d, 2H, H^3), 6.27 (d, 2H, H^5), 6.65 (dd, 2H, H^4), 7.10–7.24 (m, 10H, $H^{9,11,18,19,20}$) ppm. ^{13}C NMR (63 MHz, C_6D_6, 298 K): $\delta = 23.0$ ($C^{22,23}$), 24.5 ($C^{28,29,30,31,32,33}$), 28.8 ($C^{13,14}$), 31.2 ($C^{24,25,26,27}$), 34.9 (C^{15}), 105.5 (C^3), 116.6 (C^5), 120.8 ($C^{9,11}$), 125.0 (C^{19}), 127.2 ($C^{18,20}$), 133.5 (C^7), 140.3 (C^4), 143.1 (C^{16}), 145.1 ($C^{8,12}$), 146.8 ($C^{17,21}$), 149.4 (C^{10}), 155.9 (C^6), 169.1 (C^2) ppm.

*4.5.3. Synthesis of **4a***

CH_3Li (0.71 ml, 1.6 M, 1.13 mmol) was added slowly to **3a** (0.44 g, 0.57 mmol) in hexane (20 ml) at −30 °C. The yellow reaction mixture was allowed to warm up to room temperature and was stirred overnight as color turned into brown. LiCl was filtered off and volume of the filtrate was reduced in vacuum. Yellow crystals were obtained at room temperature after standing for 24 h. Yield: 0.32 g (52%). Elemental analyses for $C_{52}H_{64}N_4Zr$ (836.32): C, 74.7; H, 7.7; N, 6.7. Found: C, 74.0; H, 7.8; N, 6.4%.

4a: ^{1}H NMR (250 MHz, C_6D_6, 298 K): $\delta = 0.47$ (s, 6H, CH_3), 0.92 (br d, 12H, $H^{23,24/25,26}$), 1.21 (d, 12H, $H^{23,24/25,26}$), 2.15 (s, 12H, $H^{13,14}$), 3.29 (br m, 4H, $H^{21,22}$), 5.39 (d, 2H, H^3), 5.89 (d, 2H, H^5), 6.67 (dd, 2H, H^4), 7.00–7.16 (m, 12H, $H^{9,10,11,17,18,19}$) ppm. ^{13}C NMR (63 MHz, C_6D_6, 298 K): $\delta = 20.48$ ($C^{13,14}$), 23.61 ($C^{21,22}$), 28.80 ($C^{23,24/25,26}$), 28.67 ($C^{23,24/25,26}$), 54.38 (2 CH_3), 105.04 (C^3), 112.20 (C^5), 124.50 ($C^{9,11}$), 126.10 ($C^{18/10}$), 127.84 ($C^{17,19}$), 135.89 ($C^{18/10}$), 136.30 ($C^{8,12}$), 139.10 (C^7), 140.91 (C^4), 143.24 (C^{15}), 144.58 ($C^{16,20}$), 155.88 (C^6), 170.31 (C^2) ppm.

*4.5.4. Synthesis of **4b***

This compound was obtained in the same way as **4a**, with CH_3Li (0.98 ml, 1.6 M, 1.56 mmol) and **3b**, (0.84 g, 0.78 mmol) instead of **3a**. Yield: 0.49 g (61%). Elemental analyses for $C_{69}H_{99}N_4Zr$ (1075.78): C, 77.0; H, 9.3; N, 5.2. Found: C, 77.1; H, 9.2; N, 5.2%.

4b: ^{1}H NMR (250 MHz, C_6D_6, 298 K): $\delta = 0.57$ (s, 6H, CH_3), 1.11(d, 24H, $H^{24,25,26,27,28,29,30,31,32,33}$), 1.32 (d, 24H, $H^{24,25,26,27,28,29,30,31,32,33}$), 2.80–3.06 (m, 10H, $H^{13,14,15,22,23}$), 5.38 (d, 2H, H^3), 6.18 (d, 2H, H^5), 6.65 (dd, 2H, H^4), 7.11–7.19 (m, 10H, $H^{9,11,18,19,20}$) ppm. ^{13}C NMR (63 MHz, C_6D_6, 298 K): $\delta = 23.4$ ($C^{22,23}$), 24.4 ($C^{28,29,32,33}$), 24.8 ($C^{30,31}$), 26.6 ($C^{13,14}$), 31.0 ($C^{24,25,26,27}$), 34.9 (C^{15}), 55.3 (2 CH_3), 105.0 (C^3), 114.3 (C^5), 120.7 ($C^{9,11}$), 124.6 ($C^{18,20}$), 126.2 (C^{19}), 134.8 (C^4), 139.8 (C^7), 143.5 ($C^{8,12}$), 144.7 ($C^{17,21}$), 146.8 (C^{10}), 149.3 (C^{16}), 155.8 (C^6), 170.5 (C^2) ppm.

*4.5.5. Synthesis of **5a***

A Schlenk vessel was charged with amino pyridine ligand **1a**–**H** (0.106 g, 0.3 mmol) in toluene (2 ml) before trimethylaluminum solution (0.5 ml, 2.0 M Me_3Al in toluene, 1.0 mmol) was added. After stirring for 30 min all volatile was removed, to yield the corresponding, spectroscopic pure [$ApAlMe_2$] (based on ^{1}H NMR) as colorless oil in almost quantitative yield. For X-ray analysis of **5a** the residue was dissolved in 3 ml hexane. Slow evaporation of the solvent over a period of 5 days leave colorless crystals in quantitative yield. Elemental analyses for $C_{27}H_{35}AlN_2$ (414.6): C, 78.2; H, 8.5; N, 6.8. Found: C, 78.1; H, 8.6; N, 6.6%.

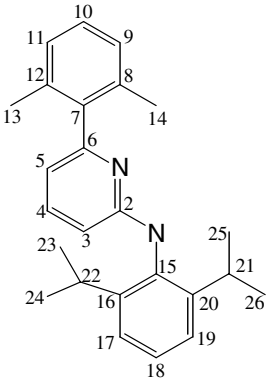

5a: ^{1}H NMR (400 MHz, C_6D_6, 298 K): $\delta = -0.35$ (s, 6H, H^{AlMe2}), 1.17 (d, 6H, $^3J(H,H) = 6.6$ Hz, H^{23-26}), 1.21 (d, 6H, $^3J(H,H) = 6.9$ Hz, H^{23-26}), 2.11 (s, 6H, $H^{13,14}$), 3.48 (sept, 1H, $^3J(H,H) = 6.9$ Hz, $H^{21,22}$), 5.58 (dd, 1H, $^3J(H,H) = 8.8$ Hz, $^4J(H,H) = 0.8$ Hz, H^3), 5.73 (dd, 1H, $^3J(H,H) = 7.0$ Hz, $^4J(H,H) = 0.8$ Hz, H^5), 6.80 (dd, 1H, $^3J(H,H) = 8.8$ Hz, $^3J(H,H) = 7.0$ Hz, H^4), 6.91 (d, 2H, $^3J(H,H) = 7.7$ Hz, $H^{9,11}$), 7.03 (t, 1H, $^3J(H,H) = 7.7$ Hz, H^{10}), 7.12–7.23 (m, 3H; H^{17-19}). ^{13}C NMR (100 MHz, C_6D_6, 298 K): $\delta = -10.2$ (br, C^{AlMe2}), 19.7 (s, $C^{13,14}$), 24.2 (s, C^{23-26}), 24.7 (s, C^{23-26}), 28.5 (s, $C^{21,22}$), 104.2 (s, C^3), 108.9 (s, C^5), 124.2 (s, $C^{17,19}$), 126.3 (s, C^{18}), 127.6 (s, $C^{9,11}$), 129.0 (s, C^{10}), 135.8 (s, $C^{8,12}$), 137.6 (s, C^7), 138.2 (s, C^{15}), 142.5 (s, C^4), 145.8 (s, $C^{16,20}$), 154.6 (s, C^6), 166.9 (s, C^2) ppm.

*4.5.6. Synthesis of **5b***

This compound was obtained in the same way as **5a**, with trimethylaluminum (0.2 ml, 2.0 M Me_3Al in toluene, 0.4 mmol) and amino pyridine ligand **1b**–**H** (0.046 g, 0.1 mmol) instead of **1a**–**H**. Yield: quantitative. Elemental analyses for $C_{34}H_{49}AlN_2$ (512.8): C, 79.6; H, 9.6; N, 5.5. Found: C, 79.4; H, 9.6; N, 5.4%.

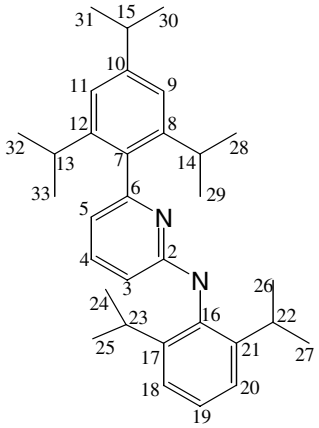

5b: ^{1}H NMR (400 MHz, C_6D_6, 298 K): $\delta = -0.24$ (s, 6H, H^{AlMe2}), 1.07 (d, 6H, $^3J(H,H) = 6.6$ Hz, H^{24-33}), 1.14 (d, 6H, $^3J(H,H) = 6.6$ Hz, H^{24-33}), 1.16 (d, 6H, $^3J(H,H) = 6.6$ Hz, H^{24-33}), 1.21 (d, 6H, $^3J(H,H) = 6.6$ Hz, H^{24-33}), 1.39 (d, 6H, $^3J(H,H) = 6.6$ Hz, $H^{28,29,32,33}$), 2.76 (sept, 1H, $^3J(H,H) = 6.6$ Hz, H^{15}), 2.90 (sept, 2H, $^3J(H,H) = 6.6$ Hz, $H^{13,14}$), 3.49 (sept, 2H, $^3J(H,H) = 6.6$ Hz, $H^{22,23}$), 5.61 (d, 1H, $^3J(H,H) = 8.8$ Hz, H^3), 6.02 (d, 1H, $^3J(H,H) = 7.3$ Hz, H^5), 6.79 (dd, 1H, $^3J(H,H) = 8.8$ Hz, $^3J(H,H) = 7.3$ Hz, H^4), 7.16 (br, 2 H, $H^{18,20}$), 7.19 (br, 3H, $H^{9,11,19}$). ^{13}C NMR (100 MHz, C_6D_6, 298 K): $\delta = -9.6$ (br, C^{AlMe2}), 23.1 ($C^{28,29,32,33}$), 24.1 (br, $C^{24-29,32,33}$), 24.2 ($C^{24,25,26,27}$), 26.1 ($C^{30,31}$), 28.5 ($C^{22,23}$), 30.9 ($C^{13,14}$), 34.7 (C^{15}), 104.3 (C^3), 111.1 (C^5), 121.0 ($C^{9,11}$), 124.2 ($C^{18,20}$), 126.3 (C^{19}), 133.1 (C^7), 138.1 (C^4), 141.6 ($C^{17,21}$), 145.7 (C^{16}), 146.9 ($C^{8,12}$), 150.1 (C^{10}), 154.9 (C^6), 167.0 ppm (C^2).

4.6. Generation of the cationic zirconium alkyl complexes

(a) Reaction with *N*,*N*-dimethylanilinium-tetra(pentafluorophenyl)borate([$PhNMe_2H$][$B(C_6F_5)_4$]): A NMR tube was charged with **4b** (0.022 g, 20 μmol), deutero-bromobenzene (0.5 ml) together with [$PhNMe_2H$][$B(C_6F_5)_4$] (0.016 g, 20 μmol). Afterwards the tube was sealed and shaken for 5 min to become a clear solution before measured.

^{1}H NMR (250 MHz, C_6D_5Br, 298 K): $\delta = 0.21$ (s, 3H, CH_3) 0.60–1.40 (m, 63H, $CH(CH_3)_2$), 2.00–3.20 (m, 10H, $CH(CH_3)_2$), 2.60 (s, 6H, $N(CH_3)_2$), 5.72 (d, 2H, H-3), 6.37 (d, 2H, H-5), 6.59 (d, 2H, PhN), 6.73 (t, 1H, PhN), 7.00–7.20 (m, 13H, H-9,11, 18, 19, 20) ppm. ^{13}C NMR (C_6D_5Br, 298 K): $\delta = 22.0$ ($CH(CH_3)_2$,C-22), 22.5 ($CH(CH_3)_2$,C-23), 23.1 ($CH(CH_3)_2$,C-28), 23.5 ($CH(CH_3)_2$, C-29), 24.1 ($CH(CH_3)_2$, C-30), 24.8 ($CH(CH_3)$, C-31), 25.8 ($CH(CH_3)_2$,C-32,33), 26.2 ($CH(CH_3)$, C-13), 28.7 ($CH(CH_3)_2$,C-14), 31.1 ($CH(CH_3)_2$, C-26,27), 31.3 ($CH(CH_3)_2$, C-24,25), 34.7 ($CH(CH_3)_2$, C15), 54.0 ($N(CH_3)_2$), 73.3 (CH_3), 107.1 (CH, C-3/5), 118.6 (CH, C-3/5), 121.4 (CH, C-9,11), 122.8 (CH, C-18,20), 126.0 ($B(C_6F_5)_4$), 126.2 (CH, C-19), 135.5 ($B(C_6F_5)_4$), 136.7 (CH, C-4), 138.9 ($B(C_6F_5)_4$), 139.0 (C, C-7), 142.6 (C, C-8,12), 144.6(C, C-17,21), 146.5 (C, C-10), 148.0 (C, C-16), 150.6 ($B(C_6F_5)_4$), 155.5 (C, C-6), 165.2 (C, C-2) ppm. ^{19}F NMR (C_6D_5Br, 298 K): $\delta = 132.1$ (*o*-F), 162.6 (*p*-F), 166.5 (*m*-F).

(b) Reaction with tris(pentafluorophenyl)borane ($B(C_6F_5)_3$): A NMR tube was charged with **4b** (0.022 g, 20 μmol), deutero-benzene (0.5 ml) together with $B(C_6F_5)_3$ (0.012 g, 22 μmol) to give a red oil, which was separated from the solvent and dissolved in deutero-bromobenzene (0.5 ml) before measured.

^{1}H NMR (250 MHz, C_6D_5Br, 298 K): $\delta = 0.21$ (s, 3H, CH_3) 0.60-1.40 (m, 63H, $CH(CH_3)_2$, CH_3B), 2.00–3.20 (m, 10H, $CH(CH_3)_2$), 5.72 (d, 2H, H-3), 6.37 (d, 2H, H-5), 6.96 (dd, 2H, H-4), 7.00–7.20 (m, 10H, H-9,11, 18, 19, 20) ppm. ^{13}C NMR (C_6D_5Br, 298 K): $\delta = 11.1$ (br, $CH_3B(C_6F_5)_3$), 22.0 ($CH(CH_3)_2$,C-22), 22.5 ($CH(CH_3)_2$,C-23), 23.1 ($CH(CH_3)_2$,C-28), 23.5 ($CH(CH_3)_2$,C-29), 24.1 ($CH(CH_3)_2$, C-30), 24.8 ($CH(CH_3)$, C-31), 25.8 ($CH(CH_3)_2$,C-32,33), 26.2 ($CH(CH_3)$, C-13), 28.7 ($CH(CH_3)_2$,C-14), 31.1 ($CH(CH_3)_2$, C-26,27), 31.3 ($CH(CH_3)_2$, C-24,25), 34.7 ($CH(CH_3)_2$, C15), 73.3 (CH_3), 107.1 (CH, C-3/5), 118.6 (CH, C-3/5), 121.4 (CH, C-9,11), 122.8 (CH, C-18,20), 125.8 ($CH_3B(C_6F_5)_3$), 126.2 (CH, C-19), 135.7 ($CH_3B(C_6F_5)_3$), 136.7 (CH, C-4), 138.6 ($CH_3B(C_6F_5)_3$), 139.0 (C, C-7), 142.6 (C, C-8,12), 144.6(C, C-17,21), 146.5 (C, C-10), 148.0 (C, C-16), 150.1 ($CH_3B(C_6F_5)_3$), 155.5 (C, C-6), 165.2 (C, C-2) ppm. ^{19}F NMR (C_6D_5Br, 298 K): $\delta = 132.2$ (*o*-F), 164.9 (t, *p*-F), 167. 2 (*m*-F).

4.7. NMR tube reaction with d-MAO

(a) A NMR tube was charged with **3a** (0.020 g, 20 μmol), deutero-bromobenzene (0.5 ml) together with d-MAO (0.029 g, 500 μmol). Afterwards the tube was sealed, shaken for 5 min and measured.

(b) A NMR tube was charged with **3b** (0.023 g, 20 μmol), deutero-bromobenzene (0.5 ml) together with d-MAO (0.029 g, 500 μmol). Afterwards the tube was sealed, shaken for 5 min and measured.

5. Supplementary material

CCDC 289175, 289174, 640085, and 640086 contain the supplementary crystallographic data for **3a**, **3b**, **5a**, and **5b**. These data can be obtained free of charge via http://www.ccdc.cam.ac.uk/conts/retrieving.html, or from the Cambridge Crystallographic Data Centre, 12 Union Road,

Cambridge CB2 1EZ, UK; fax: (+44) 1223-336-033; or e-mail: deposit@ccdc.cam.ac.uk.

Acknowledgements

We thank the Alexander von Humboldt-Stiftung (Grant for N.M.S.) and the "Fonds der Chemischen Industrie" for financial support and Anna-Maria Dietel for lab assistance and Christian Döring and Germund Glatz for assistance in the X-ray lab.

References

[1] For review on aminopyridinato ligands see: R. Kempe, Eur. J. Inorg. Chem. (2003) 791–803.
[2] For selected reviews on amidinate coordination chemistry see: (a) F.T. Edelmann, Coord. Chem. Rev. 137 (1994) 403–481;
(b) J. Barker, M. Kilner, Coord. Chem. Rev. 133 (1994) 219–300;
(c) N. Nagashima, H. Kondo, T. Hayashida, Y. Yamaguchi, M. Gondo, S. Masuda, K. Miyazaki, K. Matsubara, K. Kirchner, Coord. Chem. Rev. 245 (2003) 177–190.
[3] For selected reviews on NacNac coordination chemistry see: (a) L. Kakaliou, W.J. Scanlon IV, B. Qian, S.W. Baek, M.R. Smith III, D.H. Motry, Inorg. Chem. 38 (1999) 5964–5977;
(b) B. Qian, W.J. Scanlon IV, M.R. Smith III, D.H. Motry, Organometallics 18 (1999) 1693–1698;
(c) L . Bourget-Merle, M.F. Lappert, J.R. Severn, Chem. Rev. 102 (2002) 3031–3065.
[4] (a) M. Oberthür, G. Hillebrand, P. Arndt, R. Kempe, Chem. Ber. 130 (1997) 789–794;
(b) R. Kempe, A. Spannenberg, S. Brenner, Z. Kristallogr. 211 (1996) 497–498;
(c) R. Kempe, A. Spannenberg, S. Brenner, Z. Kristallogr. 211 (1996) 499–500;
(d) R. Kempe, A. Spannenberg, S. Brenner, Z. Kristallogr. 211 (1996) 569–570;
(e) R. Kempe, G. Hillebrand, Z. Kristallogr. 218 (2003) 569–570;
(f) C. Morton, P. O'Shaughnessy, P. Scott, Chem. Commun. (2000) 2099–2100;
(g) R. Kempe, S. Brenner, P. Arndt, Organometallics 15 (1996) 1071–1074;
(h) H. Fuhrmann, S. Brenner, P. Arndt, R. Kempe, Inorg. Chem. 35 (1996) 6742–6745;
(i) E.J. Crust, I.J. Munslow, C. Morton, P. Scott, Dalton Trans. (2004) 2257–2266;
(j) E.J. Crust, A.J. Clarke, R.J. Deeth, C. Morton, P. Scott, Dalton Trans. (2004) 4050–4058;
(k) M. Polamo, M. Leskelä, J. Chem. Soc., Dalton Trans. (1996) 4345–4349;
(l) C. Jones, P.C. Junk, S.J. Leary, N.A. Smithies, Inorg. Chem. Commun. (2003) 1126–1128.
[5] (a) N.M. Scott, T. Schareina, O. Tok, R. Kempe, Eur. J. Inorg. Chem. (2004) 3297–3304;
(b) N.M. Scott, R. Kempe, Eur. J. Inorg. Chem. (2005) 1319–1324;
(c) W.P. Kretschmer, A. Meetsma, B. Hessen, T. Schmalz, S. Qayyum, R. Kempe, Chem. Eur. J. 12 (2006) 8969–8978;
(d) W.P. Kretschmer, A. Meetsma, B. Hessen, N.M. Scott, S. Qayyum, R. Kempe, Z. Anorg. Allg. Chem. 632 (2006) 1936–1938.
[6] D.J. Arriola, E.M. Carnahan, P.D. Hustad, R.L. Kuhlman, T.T. Wenzel, Science 312 (2006) 714–719.
[7] E. Otten, P. Dijkstra, C. Visser, A. Meetsma, B. Hessen, Organometallics 24 (2005) 4374–4386.
[8] S. Deeken, G. Motz, R. Kempe, Z. Anorg. Allg. Chem. 633 (2007) 320–325.
[9] (a) A.D. Horton, J. de With, A.J. van der Linden, H. van de Weg, Organometallics 15 (1996) 2672–2674;
(b) C. Pellecchia, A. Immirzi, A. Grassi, A. Zambelli, Organometallics 12 (1993) 4473–4478;
(c) A.D. Horton, J. de With, J. Chem. Soc., Chem. Commun. (1996) 1375–1376.
[10] The term "highly active" was taken from a classification introduced by: G.J.P. Britovsek, V.C. Gibson, D.F. Wass, Angew. Chem. 111 (1999) 448–468;
Angew. Chem., Int. Ed. 38 (1999) 428–447.
[11] (a) C. Jones, P.C. Junk, S.G. Leary, N.A. Smithies, Main Group Met. Chem. 24 (2001) 383–384;
(b) M. Pfeiffer, A. Murso, L. Mahalakshmi, D. Moigno, W. Kiefer, D. Stalke, Eur. J. Inorg. Chem. (2002) 3222–3234.
[12] J. Ashenhurst, L. Brancaleon, S. Gao, W. Liu, H. Schmider, S. Wang, G. Wu, Q.G. Wu, Organometallics 17 (1998) 5334–5341.
[13] We assume a similar degree of steric protection for the dimethyl complexes as for the dichloro complexes.
[14] H.H. Brinzinger, D. Fischer, R. Mühlhaupt, B. Rieger, R.M. Waymouth, Angew. Chem. 107 (1995) 1255–1283;
Angew. Chem., Int. Ed. 34 (1995) 1143–1170.
[15] A. Tynys, T. Saarinen, K. Hakala, T. Helaja, T. Vanne, P. Lehmus, B. Löfgren, Macromol. Chem. Phys. 206 (2005) 1043–1056.
[16] (a) G.W. Coates, P.D. Hustad, S. Reinartz, Angew. Chem. 114 (2002) 2340–2361;
Angew. Chem., Int. Ed. 41 (2002) 2236–2257;
(b) G.J. Domski, J.M. Rose, G.W. Coates, A.D. Bolig, M. Brookhart, Prog. Polym. Sci. 32 (2007) 30–92.
[17] (a) P.J. Chirik, J.E. Bercaw, Organometallics 24 (2005) 5407–5423;
(b) P.J. Chirik, N.F. Dalleska, L.M. Henling, J.E. Bercaw, Organometallics 24 (2005) 2789–2794;
(c) S.F. Vyboishchikov, D.G. Musaev, R.D.J. Froese, K. Morokuma, Organometallics 20 (2001) 309–323.
[18] (a) H. Schumann, Angew. Chem. 96 (1984) 475–493;
Angew. Chem., Int. Ed. 23 (1984) 474–492;
(b) C.J. Schaverien, Adv. Organomet. Chem. 36 (1994) 283–362;
(c) H. Schumann, J.A. Messe-Marktscheffel, L. Esser, Chem. Rev. 95 (1995) 865–986;
(d) F.T. Edelmann, D.M.M. Feckmann, H. Schumann, Chem. Rev. 102 (2002) 1851–1896;
(e) S. Arndt, J. Okuda, Chem. Rev. 102 (2002) 1953–1976.
[19] L. Caporaso, L. Izzo, L. Oliva, Macromolecules 32 (1999) 7329–7331.
[20] W. Hölderich, M. Hesse, F. Näumann, Angew. Chem. 100 (1988) 232–251;
Angew. Chem., Int. Ed. 27 (1988) 226–246.
[21] J.F. van Baar, P.A. Schut, A.D. Horton, O.T. Dall, G.M.M. van Kessel, World Pat. Appl. WO 2000035974 A1, Montell Techn. Co., 2000.